

LASERS

https://doi.org/10.1070/QEL16494

Spectral and power characteristics of a 5% Tm : $KLu(WO_4)_2$ N_m-cut minislab laser passively *Q*-switched by a Cr^{2+} : ZnSe crystal

S.M. Vatnik, I.A. Vedin, P.F. Kurbatov, E.A. Smolina,
A.A. Pavlyuk, Yu.V. Korostelin, Ya.K. Skasyrsky

Abstract. **Laser characteristics of a 5%Tm : $KLu(WO_4)_2$ N_m-cut minislab laser passively *Q*-switched by a Cr^{2+} : ZnSe saturable absorber are presented. At a pump power of 21 W, the average laser power at a wavelength of 1.91 μm was 3.2 W (pulse duration 35 ns, pulse energy 0.3 mJ). The maximum slope efficiency of the laser in the *Q*-switched regime was 31%; the loss in power with respect to the cw regime did not exceed 17%. At pump powers above 15 W, the dependence of the output power in the *Q*-switched regime on the pump power considerably differed from linear, which was explained by the formation of a thermal lens in the saturable absorber volume. The experimental energies and durations of laser pulses well agree with the values calculated from rate equations.**

Keywords: *passive Q-switching, slab laser, diode pumping, thulium laser, Cr^{2+} : ZnSe saturable absorber.*

1. Introduction

Two-micron lasers are of considerable interest for a number of applications, such as ecological monitoring, medicine, and pumping of optical parametric oscillators [1–3]. Crystals and ceramics doped with trivalent thulium are promising materials for designing highly efficient lasers operating on the $^3F_4$–$^3H_6$ transition with high average and peak powers [4–6]. Optimisation of thulium concentration in active elements allows almost a twofold increase in the quantum yield upon pumping into the $^3H_6$–$^3H_4$ (~0.8 μm) due to high cross-relaxation rates [7, 8]. Diode-pumped thulium lasers have demonstrated excellent (in some cases exceeding 50%) optical efficiency in the cw and quasi-cw regimes [9–11], broad (up to 200 nm) tuning range [10, 11], and high peak powers in the passive and active *Q*-switching regimes [12–14].

It is of interest to study passive *Q*-switching (PQS) of lasers based on double potassium–rare-earth tungstates doped with trivalent thulium. Since the cross sections of the $^3F_4$–$^3H_6$ laser transitions in Tm : $KRe(WO_4)_2$ crystals (where Re is Y, Gd, or Lu) are about $(1–4) \times 10^{-20}$ см^2, which is an order of magnitude larger than the cross sections for Tm : YAG, Tm : YAP, Tm : Lu_2O_3, and other crystals [15, 16], one should expect that laser pulses in the PQS regime will be much shorter with a corresponding increase in their peak power. In particular, PQS of a Tm : $KLu(WO_4)_2$ microchip laser with an average power up to 150 mW was studied in detail in [6]; the pulse duration and peak power at wavelength $\lambda = 1.85$ μm were 0.78 ns and 33 kW, respectively. In the present work, we used PQS of a laser with a 5%Tm : KLuW minislab active element, which allowed us to increase the average laser power to several watts at a total optical efficiency of 15% and to achieve a laser pulse peak power higher than 40 kW.

S.M. Vatnik, I.A. Vedin, P.F. Kurbatov, E.A. Smolina Institute of Laser Physics, Siberian Branch, Russian Academy of Sciences, prosp. Akad. Lavrent'eva 13/3, 630090 Novosibirsk, Russia;
e-mail: vatnik@laser.nsc.ru;
A.A. Pavlyuk A.V. Nikolaev Institute of Inorganic Chemistry, Siberian Branch, Russian Academy of Sciences, prosp. Akad. Lavrent'eva 3, 630090 Novosibirsk, Russia;
Yu.V. Korostelin, Ya.K. Skasyrsky P.N. Lebedev Physical Institute, Russian Academy of Sciences, Leninsky prosp. 53, 119991 Moscow, Russia

Received 11 August 2017; revision received 13 September 2017
Kvantovaya Elektronika **47** (11) 981–985 (2017)
Translated by M.N. Basieva

2. Experiment

All experiments on PQS were performed with a potassium–lutetium double tungstate 5%Tm : $KLu(WO_4)_2$ (hereinafter 5%Tm : KLuW) active element (slab) oriented along the optical indicatrix axes with the size of 6.06 mm (axis N_m), 0.95 mm (axis N_p coinciding with crystallographic axis b [17]), and 0.24 mm (axis N_g). The slab was pumped by a collimated beam of a 40-W CS-mount laser diode bar (λ = 806 nm) through the upper antireflection-coated face with the size of 6.06×0.24 mm. A highly reflecting coating for the same (780–820 nm) spectral range was deposited onto the lower face of the slab (Fig. 1, see also Fig. 2 from [17]). In all experiments, we used a double-pass pumping scheme and determined the absorbed power as the difference between the incident and passed powers.

The saturable absorber (SA) was made of a Cr^{2+} : ZnSe single crystal grown from the vapour phase [18, 19] and had the form of a 3 × 5-mm plate 0.26 mm thick; its unsaturated absorption at the laser wavelength $\lambda \sim 1.91$ μm was 2.2% per pass. The plane-parallel faces of the SA were coated with dielectric layers with reflection coefficients R = 0.1% and 83% for $\lambda = 1.91$ μm.

The PQS regime was studied for two cavity types, A and B, shown in Fig. 1. Cavity A was formed by a highly reflecting concave cylindrical mirror with a cylinder radius of 50 mm, which compensated for the negative thermal lens in the active element, and a plane output mirror on the saturable absorber. The physical length of cavity A was 7.0 mm, i.e., the mirrors were very close to the slab faces (gap ~0.1 mm), which completely corresponded to the optical scheme of [17]. Cavity B differed from A by the presence of an intracavity fused silica lens with focal length f = +20 mm, both faces of which were antireflection coated with $R \sim 0.15$%. The highly reflecting mirror in cavity B was also placed very close to the active ele-

ment face and was either cylindrical (radius 50 mm) or plane; the distance between the mirror and the lens (~23 mm) was determined by the maximum laser power in the quasi-cw pumping regime. For experiments with cavity B, the saturable absorber was glued to a rectangular leucosapphire plate 7 × 4 × 3 mm in size with one face antireflection coated for a wavelength of 1.91 μm (see the upper inset in Fig. 2), which allowed us to improve heat removal and decrease overheating of the Cr^{2+}:ZnSe crystal in the lasing region. Since the light field propagates from the dielectric coating into a medium with a refractive index of ~1.5 (epoxy resin) rather than into the air, the transmittance of the output mirror on the saturable absorber T_{oc} slightly increased to 19%.

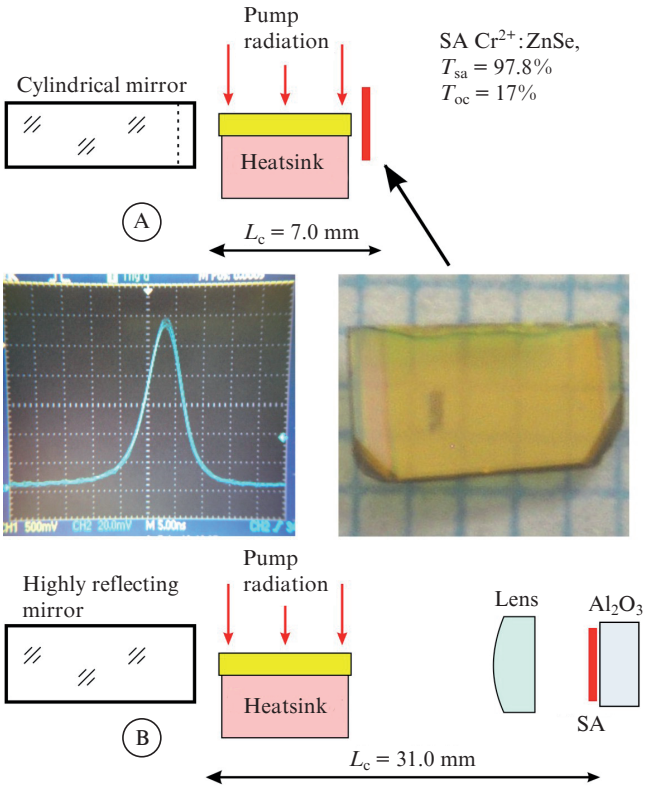

Figure 1. Schematic of cavities A and B. The left photograph shows a laser pulse for cavity A at an average pump power of 2.1 W (peak power 15 W); the pulse FWHM is 7 ns. The right photograph shows the saturable absorber after optical breakdown.

The pump and laser light powers were measured using an Ophir L30A power meter; the shape of laser pulses was recorded by a PD24-02 InGaAs photodiode and a Tektronix oscilloscope; the time resolution of the system was 1 ns. The laser spectra were recorded using an MDR-204 monochromator with a scanning rate of 1 nm min^{-1} and a PD24-10 photodiode with an almost plane dependence of the photoresponse in the range of 1.5–2.4 μm; other details of the experiment can be found in [17].

3. Results and discussion

Preliminary experiments on PQS were performed for the short cavity A upon quasi-cw pumping. The duration of current pulses injected into the laser diode bar was 7 ms at a pulse repetition rate of 50 ms, i.e., duty cycle was 0.14. The sequence

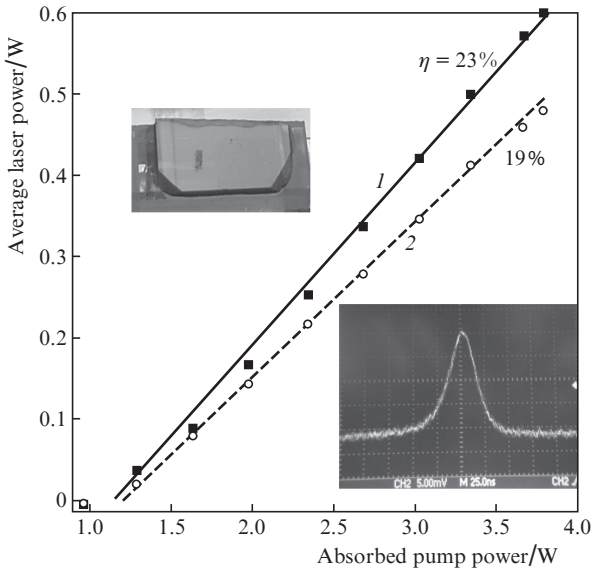

Figure 2. Dependences of the output laser power in the (*1*) quasi-cw and (*2*) PQS regimes for cavity B with a cylindrical highly reflecting mirror at diode bar current pulses with a duration of 7 ns and a repetition rate of 20 Hz. The photographs show (left) the saturable absorber on a heat-conducting leucosapphire plate and (right) a laser pulse at an average pump power of 3.8 W.

of laser pulses was stable up to an average laser power of 300 mW, at which the pulse repetition rate during pumping was 7.0 kHz (1 kHz on average) with a pulse duration of 7 ns (see photograph in Fig. 1, left). Further increase in the average pump power (above 2.3 W) led to burning-out of the coating and partial degradation of the SA (photograph in Fig. 1, right). Due to a small (100 μm) distance between the SA and slab faces, the latter was partially contaminated by the burned-out SA fragments. After thorough cleaning of the faces, the laser characteristics of the slab in cavity A were measured at the plane output mirror transmittance T_{oc} = 19% and a cavity length of 6.6 mm under conditions completely identical to the conditions of [17]. In the quasi-cw pumping regime, the slope efficiency slightly decreased, from initial 43% [17] to 41%, the lasing threshold being almost unchanged, i.e., distortions of the slab face turned out to be insignificant.

All further experiments were performed with cavity B, for which the laser fluence in the region of the SA was lower than the breakdown threshold (~1 J cm^{-2}) for all pumping regimes. Figures 2 and 3 show the laser characteristics for the cavity with a cylindrical highly reflecting mirror under quasi-cw and cw pumping. According to the data reported, the slope efficiency in the PQS regime (η = 19%) comprises 83% of the corresponding value (23%) obtained in the case of using a plane output mirror with transmittance T_{oc} = 19% instead of the SA. Note also that the laser pulse duration (τ = 35 ns, see the oscillogram in Fig. 2) increased approximately proportionally to the increase in the cavity length.

In the case of cw pumping, the dependence of the output laser power on the absorbed pump power begins to deviate from a straight line as the absorbed pump power exceeds 15 W; simultaneously, one observes considerable fluctuations of the laser pulse energy (Fig. 3). We believe that the deviation from a linear dependence is related to the formation of a thermal lens in the SA volume due to a high thermooptical coefficient of ZnSe (~65 × 10^{-6} K^{-1} [20]), which is almost two

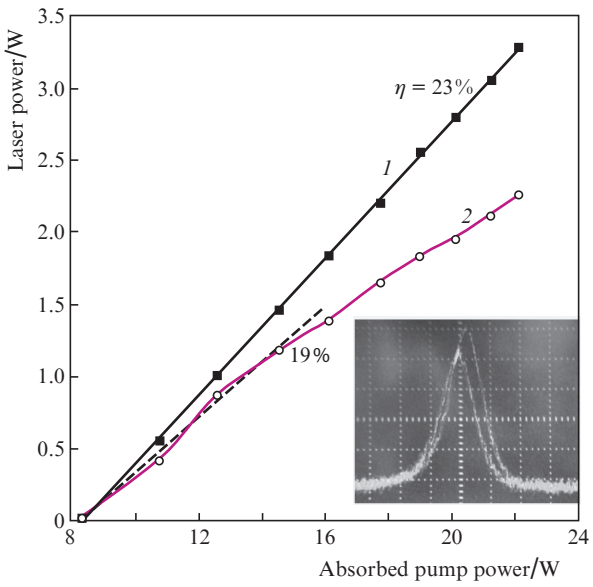

Figure 3. Laser characteristics of the slab in cavity B with a cylindrical highly reflecting mirror (*1*) under cw pumping and (*2*) in the PQS regime. The photograph shows typical instability of pulse amplitudes at the maximum absorbed pump power of 22 W.

orders of magnitude higher than that for the 5%Tm:$KLu(WO_4)_2$ crystal [17, 21] (-2×10^{-6} K^{-1}, $E\|N_p$). According to estimates of [22, 23], the focal length of the thermal lens in the SA at the maximum heat release calculated as a difference between the laser powers in the cw and PQS regimes is ~500 mm, which, taking into account two passes through the SA (~250 mm), corresponds to about 8% of the optical power of the intracavity lens with $f = +20$ mm. In this case, the relative decrease in the laser power in the PQS regime can be caused by leaving the stability region. This is also implicitly indicated by much higher instabilities of the pulse energy and duration (including, in some cases, generation of double pulses), which cannot be eliminated even by very deliberate aligning of the cavity.

Typical laser spectra in the PQS regime upon quasi-cw pumping at a maximum output power of 0.48 W are shown in Fig. 4; the spectra were recorded successively during 30 min. Similar to [17], the small differences in the spectral profiles are probably caused by a temperature drift (~1 °C) of the heat-sink base on which the diode bar, the slab, and the SA are mounted. The laser line spectral width is about 5 nm, which is somewhat smaller than the corresponding width for the cw regime without PQS (~8 nm) [17]. This spectral narrowing can be caused by competition of individual spectral lines corresponding to the local maxima on the gain profile. In this case, the dispersion of rise times of generated modes will not exceed a light pulse duration, i.e., the laser spectrum will be shorter than in the cw regime [24].

The replacement of the cylindrical highly reflecting mirror by a plane mirror in cavity B (Fig. 1) leads to a considerable increase in the slope efficiency and output laser power (Figs 5 and 6). Like in the previous case (see Figs 3, 4), the slope efficiencies in the PQS regime are almost the same for quasi-cw and cw pumping at low pump powers, while an increase in the cw pump power above 15 W also causes a noticeable decline of the output power. The breakdown threshold (burnout of the active element face) was achieved at an absorbed pump

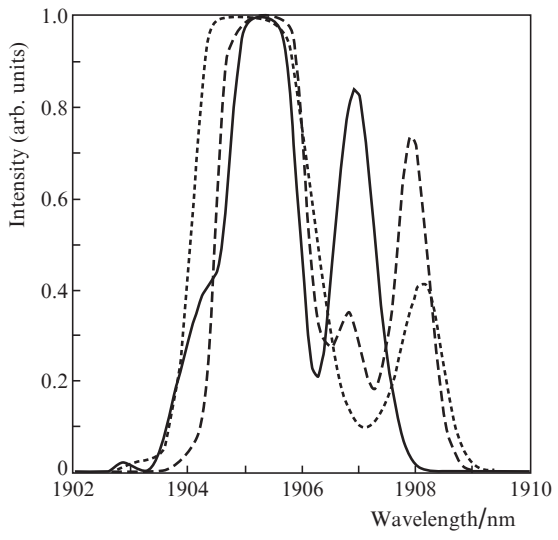

Figure 4. Typical laser spectra for cavity B with a cylindrical highly reflecting mirror at an average quasi-cw (7 ms/50 ms) pump power of 3.8 W.

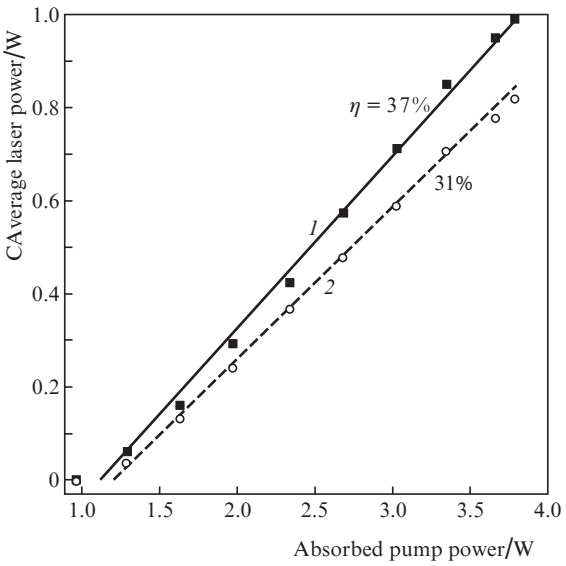

Figure 5. Dependences of the average output laser power on the average pump power in (*1*) quasi-cw and (*2*) PQS regimes for cavity B with a cylindrical highly reflecting mirror at diode bar current pulses with a duration of 7 ns and a repetition rate of 20 Hz; duty cycle is 0.14.

power of 22 W, while the average output power at a pump power of 21 W in the PQS regime was 3.2 W.

The dynamic characteristics of laser pulses in the PQS regime were analysed in the approximation of rate equations similar to those given in [25, 26]:

$$\frac{dN_2}{dt} = \eta Q - \frac{N_2}{\tau_{Tm}} - 2c\Phi[(\sigma_e + \sigma_a)N_2 - \sigma_a N], \quad (1)$$

$$\frac{d\Phi}{dt} =$$

$$\frac{2c\Phi[(\sigma_e+\sigma_a)N_2 - \sigma_a N]L_{ae} - c\Phi[T_{oc}+2\sigma_{sa}(n-n_2)L_{sa}]}{L}, \quad (2)$$

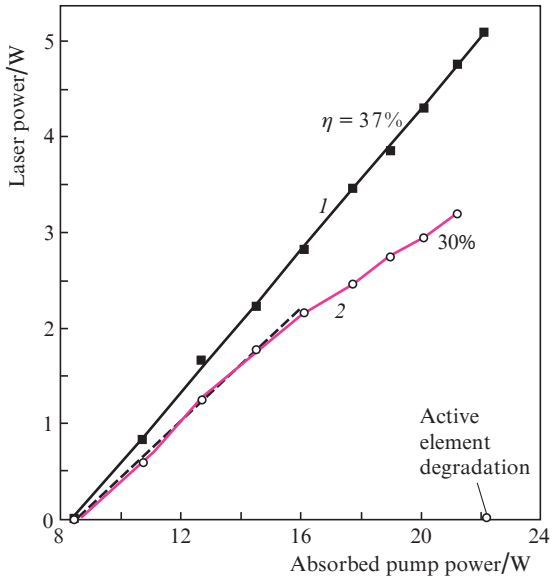

Figure 6. Laser characteristics of the slab in cavity B with a cylindrical highly reflecting mirror (*1*) under cw pumping and (*2*) in the PQS regime.

$$\frac{dn_2}{dt} = 2c\Phi\sigma_{sa}(n - n_2) - \frac{n_2}{\tau_{Cr}}, \quad (3)$$

where N_2 is the volume density of thulium ions on the $^3F_4$ upper laser level, t it time, η is the laser slope efficiency, $Q = P\chi/(\hbar\omega V)$ is the volume pump rate, P and $\hbar\omega$ are the pump photon power and energy; χ is the efficiency of the pump photon conversion into the $^3F_4$ level population (at a 5% thulium concentration, $\chi \sim 1.9$), V is the slab volume, τ_{Tm} is the lifetime of the $^3F_4$ upper laser level, c is the speed of light, Φ is the volume density of photons in the cavity, σ_e and σ_a are the cross sections of radiative and absorption transitions of thulium ions at the laser wavelength, N is the concentration of thulium ions in the crystal, L_{ae} is the active element length, T_{oc} is the output mirror transmittance, σ_{sa} is the cross section of the transition from the ground $^5T_2$ state of Cr^{2+} ions in the saturable absorber, n and n_2 are the concentration of Cr^{2+} in the ZnSe crystal and the volume density of Cr^{2+} ions at the ^5E level [25], L_{sa} is the saturable absorber thickness, L is the optical length of the cavity, and τ_{Cr} is the lifetime of the metastable ^5E level.

Equations (1)–(3) were analysed by numerical methods. Since all the basic parameters of the equations (cavity length, geometric dimensions of the slab, cross sections of all transitions, lifetimes of levels, etc.) are either determined by the experimental conditions or known from publications [10, 27], one can directly calculate the laser pulse characteristics in the PQS regime. Comparison with experiment showed that, if we use the value $\sigma_{sa}nL_{sa} = 2.2\%$ found from spectral measurements as the unsaturated SA absorption, the calculated durations and repetition rates of laser pulses for both cavity types (A and B) will be underestimated approximately by a factor of two with respect to experiment, while the pulse energy will be overestimated by the same factor. This circumstance can be explained by the fact that the measured losses in the passive Q-switch are composed of both unsaturated absorption by Cr^{2+} ions and scattering from crystal defects and other inhomogeneities, including surface treatment defects. Taking this into account, the value of unsaturated absorption $\sigma_{sa}nL_{sa}$ of the Cr^{2+}:ZnSe crystal was varied within the range of 1.0%–2.0%, and the best coincidence of pulse energies and repetition rates with experimental values was obtained for $\sigma_{sa}nL_{sa} = 1.35\%$, i.e., the residual losses in the SA were 0.85% (Table 1).

Lower losses (0.79%) are obtained from the condition of equality of the experimental and calculated durations of laser pulses; the calculated pulse energies and repetition rates in this case differ from experimental by 15%. In general, according to the reported data, the system of rate equations (1)–(3) makes it possible to rather correctly describe the formation kinetics and the main parameters of laser pulses. A slight (10%–15%) difference between the experimental and calculated data is apparently related to the simplifying assumption that the radiation intensity distribution over the laser beam cross section is homogeneous. The account for the real light beam profile in the cavity will provide the possibility to more precisely describe both the formation of laser pulses and their characteristics.

4. Conclusions

A record-high (31%) slope efficiency of a 5%Tm:KLuW slab laser under conditions of passive Q-switching by a Cr^{2+}:ZnSe saturable absorber is demonstrated. Multiwatt lasing is achieved with a total optical efficiency of ~15% with respect to the absorbed pump power and a pulse energy of 0.3 mJ. The output power and efficiency of the passively Q-switched laser under cw pumping can be considerably increased by optimisation of the SA parameters and corresponding correction of thermal lenses formed in the active element and the Cr^{2+}:ZnSe crystal.

Acknowledgements. This work was supported by the Presidium of the Russian Academy of Sciences ('Fundamentals of Innovative Dual-Purpose Technologies for National Security' Programme, Project No. 0307-2014-0029) and by the Russian Foundation for Basic Research (Grant No. 16-52-00040).

References

1. Gibert F., Flamant P.H., Bruneau D. *Appl. Opt.*, **45**, 4448 (2006).

Table 1. Calculated and experimental results for cavities A and B under quasi-cw pumping (average power 2.1 W, peak power 15 W); $\sigma_{sa}nL_{sa} = 1.35\%$.

Cavity type	L/mm	Pulse energy/mJ	Pulse duration/ns	Pulse repetition rate/kHz
		Experiment/Calculation	Experiment/Calculation	Experiment/Calculation
A ($T_{oc} = 17\%$)	7.0	0.30/0.30	7.0/8.3	7.0*/6.9*
B ($T_{oc} = 19\%$)	31.0	0.30/0.30	35/42	6.3*/6.25*

* – during pumping.

2. Michalska M., Brojek W., Rybak Z. *Laser Phys. Lett*., **13**, 115101 (2016).
3. Haakestad M.W., Fonnum H., Lippert E. *Opt. Express*, **22**, 8556 (2014).
4. Antipov O.L., Golovkin S.Yu., Gorshkov O.N. *Quantum Electron*., **41**, 846 (2011) [*Kvantovaya Elektron*., **41**, 846 (2011)].
5. Strauss H.J., Esser M.J.D., King G., Maweza L. *Opt. Mater. Express*, **2**, 1165 (2012).
6. Loiko P., Serres J.M., Mateos X., Yumashev K.V., Yasukevich A., Petrov V., Griebner U., Aguilo M., Dıas F. *Opt. Lett*., **22**, 5220 (2015).
7. Rustad G., Stenersen K. *IEEE J. Quantum Electron*., **32**, 1645 (1996).
8. Silvestre O., Pujol M.C., Rico M., Guell F., Aguilo M., Diaz F. *Appl. Phys*. *B*, **87**, 707 (2007).
9. Vatnik S.M., Vedin I.A., Kurbatov P.F., Pavlyuk A.A. *Quantum Electron*., **44**, 989 (2014) [*Kvantovaya Elektron*., **44**, 989 (2014)].
10. Mateos X., Petrov V., Liu J., Pujol M.C., Griebner U., Aguilo M., Diaz F., Galan M., Viera G. *IEEE J. Quantum Electron*., **42**, 1008, (2006).
11. Silvestre O., Pujol M.C., Aguilo M., Diaz F., Mateos X., Petrov V., Griebner U. *IEEE J. Quantum Electron*., **43**, 257 (2007).
12. Tsai T.-Y., Birnbaum M. *Appl. Opt*., **40**, 6633 (2001).
13. Lin Jin, Pian Liu, Xuan Liu, Haitao Huang, Weichao Yao, Deyuan Shen. *Opt. Commun*., **372**, 241 (2016).
14. Yu H., Petrov V., Griebner U., Parisi D., Veronesi S., Tonelli M. *Opt. Lett*., **37**, 2544 (2012).
15. Payne S.A., Chase L.L., Smith L.K., Kway W.L., Krupke W.F. *IEEE J. Quantum Electron*., **28**, 2619 (1992).
16. Rustad G., Stenersen K. *IEEE J. Quantum Electron*., **32**, 1645 (1996).
17. Vatnik S.M., Vedin I.A., Pavlyuk A.A. *Laser Phys. Lett*., **9**, 765 (2012).
18. Kozlovskii V.I., Korostelin Yu.V., Landman A.I., Podmar'kov Yu.P., Frolov M.P. *Quantum Electron*., **33**, 408 (2003) [*Kvantovaya Elektron*., **33**, 408 (2003)].
19. Korostelin Y.V., Kozlovsky V.I. *Phys. Stat. Sol. B*, **229**, 5 (2002).
20. Harris R.J., Johnston G.T., Kepple G.A., Krok P.C., Mukai H. *Appl. Opt*., **16**, 436 (1977).
21. Loiko P.A., Vatnik S.M., Vedin I.A., Pavlyuk A.A., Yumashev K.V., Kuleshov N.V. *Laser Phys. Lett*., **10**, 125005 (2013).
22. Vatnik S.M. *Opt. Commun*., **197**, 375 (2001).
23. Vatnik S.M., El-Agmy R., Graf Th. *J. Modern Opt*., **49**, 2059 (2002)
24. Anokhov S.P., Marusii T.Ya., Soskin M.S. *Perestraivaemye lazery* (Tuneable Lasers) (Moscow: Radio i svyaz', 1982).
25. Tsai T.-Y., Birnbaum M. *Appl. Opt*., **40**, 6633 (2001).
26. Serres Y.M., Loiko P.A., Mateos X., Jambunathan V., Yasukevich A.S., Yumashev K.V., Petrov V., Griebner U., Aguilo M., Diaz F. *Appl. Opt*., **55**, 3757 (2016).
27. Petrov V., Pujol M.-C., Mateos X., Silvestre O., Rivier S., Aguilo M., Sole R.-M., Liu J., Griebner U., Diaz F. *Laser Photon. Rev*., **1**, 179 (2007).